

Slope Stability Analysis of Jointed Rock Using Distinct Element Method

L. J. LORIG, R. D. HART, AND P. A. CUNDALL

The fundamental objective in designing most slopes is to achieve the steepest slope possible consistent with knowledge of material properties, site constraints, external loads, required safety factors, and so on. Most traditional design methods for slopes in jointed media involve two-dimensional limit equilibrium analyses. All limit equilibrium analyses are restricted to predefined failure modes and assume that failure occurs along the failure surface according to a perfectly plastic shear force law (i.e., shear force is independent of displacement). Such approaches may yield reasonable results for situations in which the failure mode is readily identifiable and involves only translation or rotation. However, for more complicated problems or problems in which displacement estimates are important, limit equilibrium methods may not be appropriate. For example, in analysis of slopes composed of distinct rock blocks, analysis based on the distinct element method may be more appropriate. The results of several slope stability analyses are presented, including one actual problem in which limit analysis falsely predicts stable equilibrium and a distinct element kinematic analysis correctly predicts instability. Such false predictions can arise from the assumption of an inappropriate failure mode in limit equilibrium analysis. The distinct element method was developed specifically to study the behavior of jointed rock. Failure modes are not prescribed using this method but evolve naturally as the solution progresses. The method models a rock mass as an assemblage of blocks, not as an equivalent continuum. Discontinuities are regarded as distinct interactions between blocks with joint behavior prescribed for these interactions. A description of the fundamentals of the distinct element method relevant to slope stability analysis is included. Extensions of the method that allow practically meaningful problems to be addressed are also described. All of the features are described through illustrative examples.

Because the behavior of many rock slopes is dominated by displacements induced along joints and discontinuities (i.e., faults, bedding planes, etc.), appropriate analysis methods must account for these displacements. Current analysis methods include limit equilibrium, continuum (i.e., finite element and finite difference), and discontinuum methods.

Limit equilibrium methods assume that failure occurs along predefined failure surfaces with a perfectly plastic shear force law. This means that the shear force on the failure surface is independent of displacement. Hence, shear forces all become known functions of normal forces, and the system becomes statically determinate, although assumptions about lines of action are usually necessary. Stability in the limit equilibrium method is usually determined by a comparison of forces (i.e., driving and resisting) for a particular failure mode. The limit

equilibrium method, therefore, yields reasonable results for situations in which the failure mode is simple and readily identifiable. However, the method may be inadequate for more complicated problems or for problems in which displacements must be known (e.g., in designing reinforcement systems).

Continuum methods require that the rock mass be represented as a continuous body. Continuum methods account for the presence of discontinuities by an equivalent continuum representation. Now, equivalent continuum models can give only a limited representation for the behavior of jointed rock, that is, they cannot fully account for the various displacements associated with jointed media, such as sliding, separation, and rotation along joints. Attempts to overcome this restriction usually involve incorporating joint elements, slidelines, or interfaces to model discontinuities. However, these adaptations are usually limited by (a) the number of joints that may be considered, (b) the extent to which joints may intersect, (c) the amount of displacement that may be considered, or (d) computational inefficiencies resulting from the underlying assumption of continuum behavior.

Discontinuum methods are numerical techniques formulated specifically to analyze the behavior of discontinuous or particulate systems. The best-known and most-advanced discontinuum method is the distinct element method, which was conceived as a means to model the progressive failure of rock slopes (1). The distinct element method is not very different from other numerical methods, particularly when existing variations are considered, but three attributes are usually associated with it: first, the rock mass is composed of individual blocks that can undergo large rotation and large displacements relative to one another; second, interaction forces between blocks arise from changes in their relative geometrical configuration; and third, the solution scheme is explicit in time.

Because of these features, the distinct element method is particularly well suited to investigate problems that address the question of stability of discontinuous rock slopes. The important points of the distinct element formulation as it relates to rock slope stability are the following:

1. Both stability and instability are modeled (when a net force exists on a block, it accelerates and moves to a new position; if the forces on a block balance, it remains at rest or moves with constant velocity).
2. Forces arise between two blocks where they interact.
3. The calculation marches from one state to another in small (usually, fictitious) time increments. The "final solution" may be equilibrium, or it may be a state of continuing motion.

The following problem illustrates the distinct element analysis of a slope failure mechanism that cannot be identified from traditional slope stability analyses. The rock slope shown in Figure 1 is 40 m high with bedding that dips at an angle of 76 degrees and has a 4-m spacing. Two nearly horizontal joints intersect the slope face at a dip angle of 2.5 degrees. The friction angle of all joints is assumed to be 6 degrees. On the basis of a conventional rock slope stability analysis, this slope would be considered stable. In fact, the slope fails in a reverse-toppling mode, as shown in Figure 1. A similar analysis was performed by Cundall (2) to explain an actual slope failure at the Valdez pipeline terminal in Alaska.

DISTINCT ELEMENT FORMULATION

The essential feature of the distinct element method is its ability to model the arbitrary motion of each block with respect to any other. Blocks may be rigid or deformable. Because most slope stability problems involve stresses that are relatively low compared with the block strength and deformability, the blocks are usually considered rigid. The description of the formulation that follows has been implemented in two computer programs: Universal Distinct Element Code (UDEC) is a two-dimensional distinct element code; 3-Dimensional Distinct Element Code (3DEC) is a three-dimensional distinct element code. A detailed description of UDEC is given elsewhere (3). Hart et al. (4) describe the 3DEC formulation. For simplicity, the following discussion is based on the two-dimensional formulation.

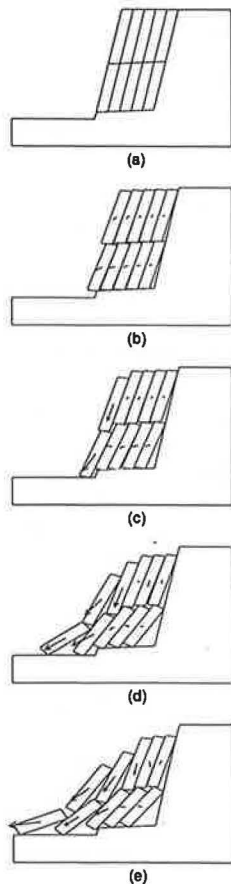


FIGURE 1 Stages in failure of slope by reverse toppling.

Calculation Cycle

The distinct element method is based on a dynamic (time domain) algorithm that solves the equations of motion of the block system by an explicit finite difference method. Cundall (5) demonstrates that such a solution scheme is better suited to indicate potential failure modes of discontinuous systems than schemes that ignore velocities and inertial forces. In the distinct element method, the motion laws and joint constitutive relations are applied at each time step. The integration of the motion law provides the new block positions and, therefore, the joint displacement increments (or velocities). Blocks are assumed to interact at discrete points referred to as "contacts." A force-displacement relation describing joint behavior at contacts is then used to obtain forces that are applied to the blocks at the next time step. The calculation cycles for rigid and deformable blocks are illustrated in Figure 2.

Block Motion

The equations of translational motion for one rigid block can be expressed as

$$\ddot{u}_i + \alpha \dot{u}_i = \frac{\sum F_i}{m} + g_i \quad (1)$$

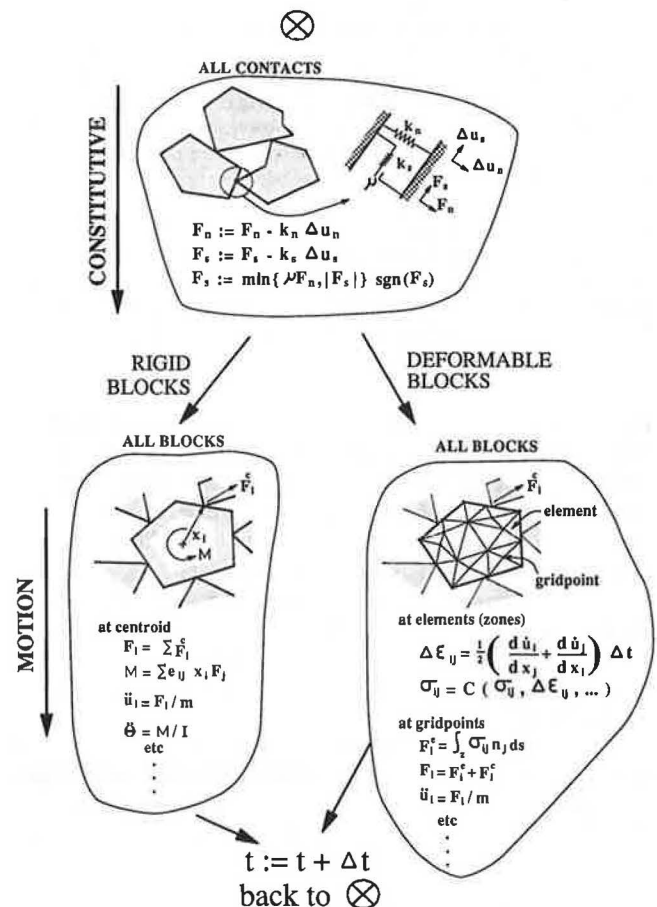


FIGURE 2 Calculation cycle used in distinct element method.

where

- \ddot{u}_i = acceleration of the block centroid,
- α = viscous (mass-proportional) damping constant,
- $\sum F_i$ = sum of forces acting on the block (from the block contacts and applied external forces),
- m = block mass, and
- g_i = gravitational acceleration.

Equation 1 is expressed in finite difference form as

$$\dot{u}_i^{(t+\Delta t/2)} = \left\{ D_1 \dot{u}_i^{(t-\Delta t/2)} + \left[\frac{\sum F_i^{(t)}}{m} + g_i \right] \Delta t \right\} D_2 \quad (2)$$

where

$$D_1 = 1 - \left(\alpha \frac{\Delta t}{2} \right),$$

$$D_2 = \frac{1}{1 + \left(\alpha \frac{\Delta t}{2} \right)}, \text{ and}$$

Δt = time step.

The equation of motion for rotation is given by

$$\dot{w}_i + \alpha w_i = \frac{M_i}{I} \quad (3)$$

where

- w_i = rotational velocity,
- M_i = total torque, and
- I = moment of inertia.

The rotation equation is integrated by finite differences in exactly the same way as the translational equations.

Contact Force

The deformability and strength properties of joints are represented in the numerical model by spring-slider elements located at contact points between a block corner and an adjacent block edge. A simple force-displacement law relates normal forces directly to the amount of notional penetration—that is,

$$F_n = k_n u_n \quad (4)$$

where

- F_n = normal force at the contact,
- k_n = normal stiffness at a point, and
- u_n = total normal penetration.

For most slope stability analyses (and all those reported here), it is assumed that the tensile strength of joints is zero.

Shear forces are considered to depend on load path. Incremental shear forces develop in proportion to incremental changes in relative shear displacement—that is,

$$\Delta F_s = k_s \Delta u_s \quad (5)$$

where

- ΔF_s = change in shear force,
- k_s = shear stiffness at a point, and
- Δu_s = incremental shear displacement.

The maximum shear force is limited according to the Mohr-Coulomb criterion

$$|F_s| \leq c + F_n \tan \phi \quad (6)$$

where c is the cohesion and ϕ is the basic joint friction angle.

Shear failure occurs when the shear force reaches the maximum value. For the work described here, joint cohesion is assumed to be zero.

In addition to point contacts specified by force-displacement relations, edge contacts are important physically because they correspond to the case of an interface closed along its entire length. For such cases, the previous expressions are written in terms of stress rather than force and representative lengths are taken into account. Because the distinct element method is based on an explicit formulation, more-realistic joint constitutive relations may be introduced. In general, the joint constitutive relations must provide the stress increments as a function of displacement increments, current stresses, and possibly other state parameters.

$$\Delta \sigma_n, \Delta \sigma_s = f(\Delta u_n, \Delta u_s, \sigma_n, \sigma_s, \dots) \quad (7)$$

One such model is the continuously yielding joint model. This model, described by Cundall and Lemos (6) and Lemos (7) is intended to simulate the intrinsic mechanism of progressive damage of a joint under shear. The continuously yielding joint model is capable, therefore, of simulating a peak-residual type of behavior.

ROCK REINFORCEMENT

The function of rock reinforcement is to mobilize forces in the interior of the rock mass that act to resist deformation. Appropriate analysis of rock reinforcement must take into account the manner in which loads are mobilized in reinforcement elements by relative displacement between rock blocks and components of the rock reinforcement.

Several types of reinforcement are designed to operate effectively in a range of ground conditions. One type is represented by a reinforcing bar or bolt fully encapsulated in a strong, stiff resin or grout. This system is characterized by the relatively large axial resistance to extensions that can be developed over a relatively short length of the shank of the bolt and by the high resistance to shear that can be developed by an element penetrating a slipping joint. A second type of reinforcement system, represented by cement-grouted cables or tendons, offers little resistance to joint shear, and development of full-axial load may require deformation of the grout over a substantial length of the reinforcing element. These two types are identified, respectively, as local reinforcement and spatially extensive reinforcement.

Formulations representing both types of reinforcement and their implementations in explicit finite difference codes are described by Brady and Lorig (8). In this paper, only local reinforcement is described and demonstrated, although both have been implemented in the distinct element method.

Local Reinforcement at Joints

In the analysis of local reinforcement, attention is focused on the loads mobilized in the reinforcement element by slip and separation at a joint. The analysis involves deformation of an active length of the element, as shown in Figure 3, a procedure justified by the experimental observations of Bjurstrom (9) and Pells (10) that, in discontinuous rock, reinforcement deformation is concentrated near an active joint.

The conceptual model of the local operation of the active length is considered in terms of two springs: one parallel to the local axis of the element, and one perpendicular to it. When shear occurs at the joint, the axial spring remains parallel to the new orientation of the active length, and the shear spring is taken to remain perpendicular to the original axial orientation. Displacements normal to the joint are accompanied by analogous changes in the spring orientations.

Illustrative Example

To illustrate the use of the local reinforcement model in the distinct element method, the problem shown in Figure 1 is repeated with the reinforcement pattern shown in Figure 4 (top) installed. Figure 4 (bottom) shows that the specified reinforcement stabilizes the slope, and it shows the loads mobilized in the reinforcement, where it crosses a discontinuity.

HYDROMECHANICAL BEHAVIOR

Hydromechanical behavior of jointed rock masses involves complex interactions between joint deformation and effective stress, causing changes in aperture and thus hydraulic conductivity. Because most rocks have low permeability, the hydraulic behavior of any rock mass is mainly determined by

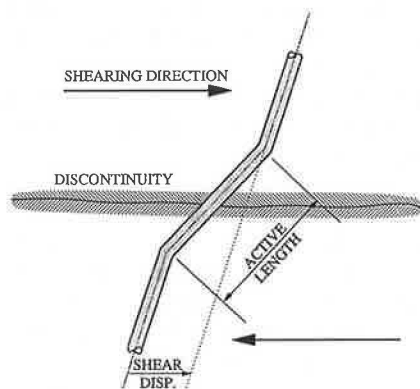


FIGURE 3 Local reinforcement deformation associated with active length of bolt.

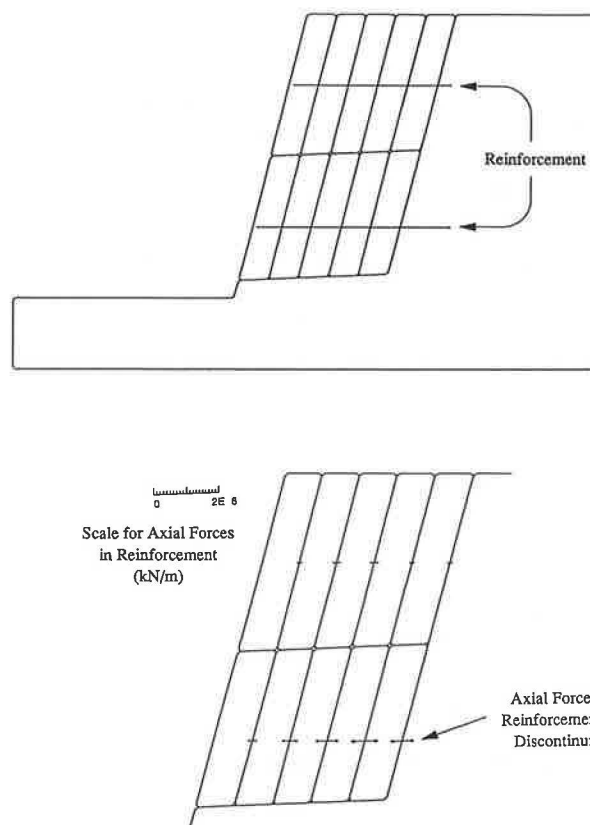


FIGURE 4 Stabilization of slope in Figure 1 by reinforcement: top, location; bottom, axial forces developed (maximum force = 830 kN).

the jointing pattern that introduces a strong directional conductivity. To the authors' knowledge, UDEC is the only general purpose distinct element code capable of performing a fully coupled mechanical-hydraulic analysis in which fracture conductivity is dependent on mechanical behavior.

Formulation

In UDEC, blocks are viewed as defining a network of interconnected voids and channels referred to as "domains." Referring to Figure 5, contacts are A-F and domains are 1-5. Domains 1, 3, and 4 represent joints, Domain 2 is located at the intersection of two joints, and Domain 5 is a void space. Flow is governed by the pressure differential (Δp) between adjacent domains. The flow rate (q) in joints is given by

$$q = ba^3 \frac{\Delta p}{l} \quad (8)$$

where

- b = joint permeability factor (whose theoretical value is $1/12\mu$, μ being the dynamic viscosity of the fluid),
- a = contact hydraulic aperture, and
- l = length assigned to the contact between the domains.

At each time step, mechanical computations determine the geometry of the system, thus yielding new values of apertures

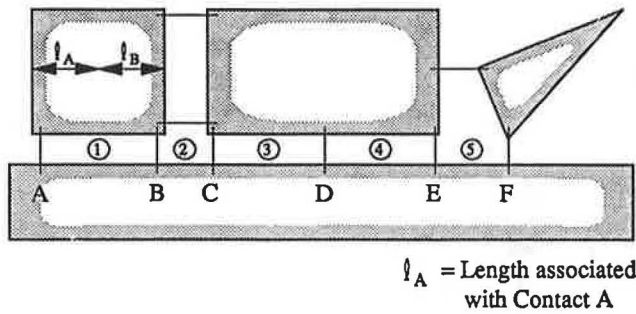


FIGURE 5 Definition of domains used in UDEC.

for all contacts and volumes of all domains. Flow rates through the contacts can then be calculated on the basis of the aforementioned formulas. Then domain pressures are updated, taking into account the net flow into the domain and possible changes in domain volume due to the incremental motion of the surrounding blocks. The new domain pressure (p) becomes

$$p = p_o + K_w Q \frac{\Delta t}{V} - K_w \frac{\Delta V}{V_m} \quad (9)$$

where

p_o = domain pressure in the preceding timestep,

Q = sum of flow rates in to the domain from all surrounding contacts,

K_w = bulk modulus of the fluid, and

$$\Delta V = V - V_o, V_m = \frac{V + V_o}{2}$$

where V and V_o are the new and old domain areas, respectively.

Given the new domain pressures, the forces exerted by the fluid on the edges of the surrounding blocks can be obtained. These forces are then added to the other forces to be applied to the block, such as the mechanical contact forces and external loads. As a consequence of this procedure, for deformable blocks, total stresses exist inside the impermeable (deformable) blocks, and effective normal stresses are obtained for the mechanical contacts.

Illustrative Example

In the example problem discussed here, the effect of various water levels behind a slope in regularly jointed rock (see Figure 6) is examined in terms of the stability of the slope. Initially, the problem is consolidated under gravity. Next, the water level at the right-hand side is raised to 6 m above the slope toe. The water level on the left-hand side is maintained at the level of the slope toe. With this right-hand water level, the slope is stable. The steady-state flow pattern for this condition is shown in Figure 7. Next, the right-hand water level is raised to 9 m. When the water level is raised, the slope remains stable. The steady-state flow condition for the 9-m water height is shown in Figure 8. Finally, the water level is raised to the top of the slope. The flow pattern for this case is shown in Figure 9. With the water level at 10 m, the lower portion of the slope slides, as shown in Figure 10. In Figures

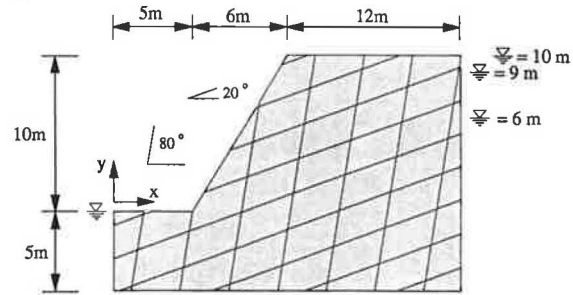


FIGURE 6 Problem geometry for example illustrating flow through jointed rock slope; $\phi = 25$ degrees, $c = 0$, $\rho = 2500 \text{ kg/m}^3$.

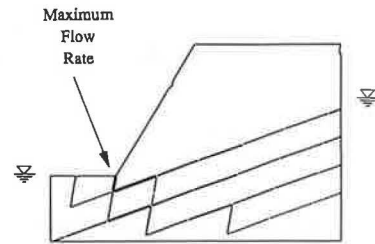


FIGURE 7 Calculated steady-state fluid flow rates for problem in Figure 5 for 6-m water level on right-hand side (maximum flow rate = $5.6e - 5 \text{ m}^3/\text{sec}$).

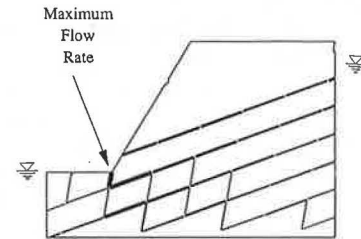


FIGURE 8 Calculated steady-state fluid flow rates for problem in Figure 5 for 9-m water level on right-hand side (maximum flow rate = $8.1e - 5 \text{ m}^3/\text{sec}$).

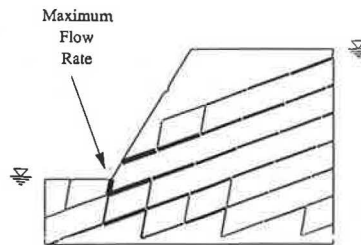


FIGURE 9 Calculated steady-state fluid flow rates for problem in Figure 5 for 10-m water level on right-hand side (maximum flow rate = $9.4e - 5 \text{ m}^3/\text{sec}$).

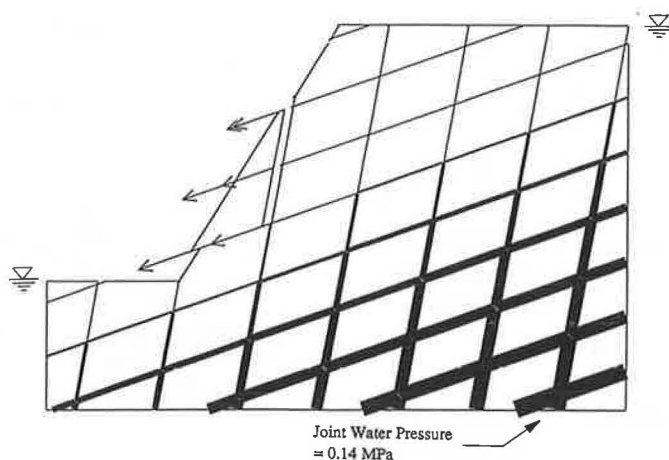


FIGURE 10 Failure of lower portion of slope when water level on right-hand side is 10 m.

7–9 the line thickness is proportional to the flow rates, and flow rates less than $1\text{e} - 5\text{ m}^3/\text{sec}$ are not shown. In Figure 10 line thickness is proportional to calculated pore pressures in joints and the maximum joint water pressure is 0.14 MPa.

DYNAMIC ANALYSIS

The stability of rock slopes subjected to earthquake motion is frequently treated as a pseudostatic (actually, pseudodynamic) limit equilibrium problem with horizontal forces applied through the centers of gravity of potential sliding blocks. The magnitudes of the forces are equal to the product of the seismic coefficient and the weights of the sliding bodies. However, such approaches do not indicate the magnitude of displacements that may develop. Displacement estimates in the slope are often necessary to assess whether the relative displacements are sufficient to significantly reduce the shear strength along a discontinuity. The Newmark method of analysis (11) furnishes an estimate of displacement, but it is based on a single sliding block. More complicated slip patterns can be modeled by the distinct element method, which also accounts for the combined effect of horizontal and vertical seismic motion. Vertical motion can change joint normal stress and thereby influence sliding.

Dynamic analyses with the distinct element method are done with reduced or zero mass damping, but stiffness-proportional damping at contacts between blocks is usually present. Damping parameters are selected in an effort to reproduce the damping of natural materials at the correct level (about 2 to 5 percent) for the important frequencies in the problem. Input records of velocity are applied to the base of the model. Both horizontal and vertical motions may be prescribed, and all analyses are performed in the time domain. Detailed procedures for performing dynamic analyses are given by Lemos and Cundall (12). These authors present dynamic analysis of dam and jointed rock foundations subject to earthquake loading. They include results that quantify the damage on joint surfaces associated with repeated cyclic loading.

In the following example, the problem geometry shown in Figure 11 is used. Horizontal and vertical motion were spec-

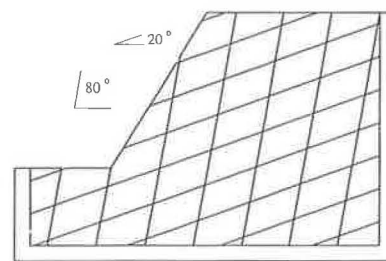


FIGURE 11 Problem geometry for example showing dynamic analysis (velocity input is specified for U-shaped base block); $\phi = 25$ degrees, $c = 0$, $\rho = 2500\text{ kg/m}^3$.

ified for the base block and the slope response observed. The dynamic excitation used in all runs is that of an actual earthquake. The velocity records shown in Figures 12 and 13 were scaled to study the effect of different earthquake magnitudes. The slope configurations after 50 sec for scaling factors of 0.1, 0.5, and 0.6 are shown in Figure 14. Figure 14a shows that the slope is essentially stable for a scaling factor of 0.1, although small permanent deformations take place. Figure 14b shows more permanent deformation, and it shows that one block has fallen to the slope toe. Figure 14c shows the greatest displacement of slope blocks. Two of the blocks have moved outside the original problem window and are not shown.

BLOCK DEFORMABILITY

Discussion so far has been limited to cases in which blocks can be assumed to be rigid. However, in some cases block deformability must be properly accounted for. The most obvious situations involve problems with high stresses relative to block strength. Another class of problems in which block deformability is important involves rock slopes or fills composed of many particles. Strictly speaking, their behavior on a small scale is that of a discontinuum. However, in cases in which particle size is small relative to critical dimensions of the problem, continuum behavior may be a reasonable ap-

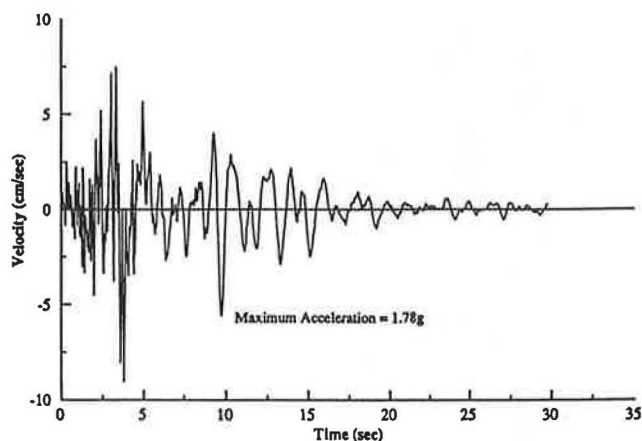


FIGURE 12 Earthquake velocity records applied to base block in Figure 11, vertical velocity input.

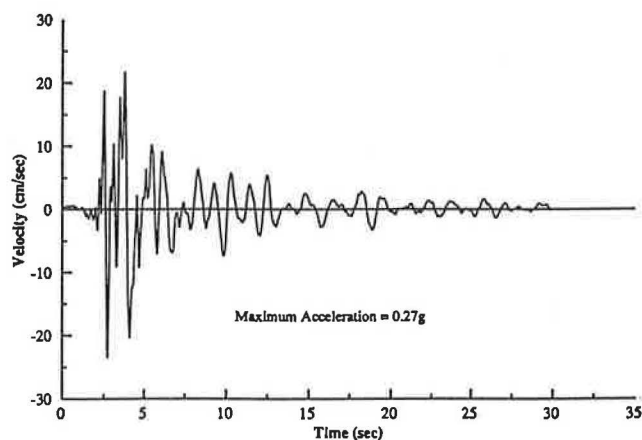


FIGURE 13 Earthquake velocity records applied to base block in Figure 11, horizontal velocity input.

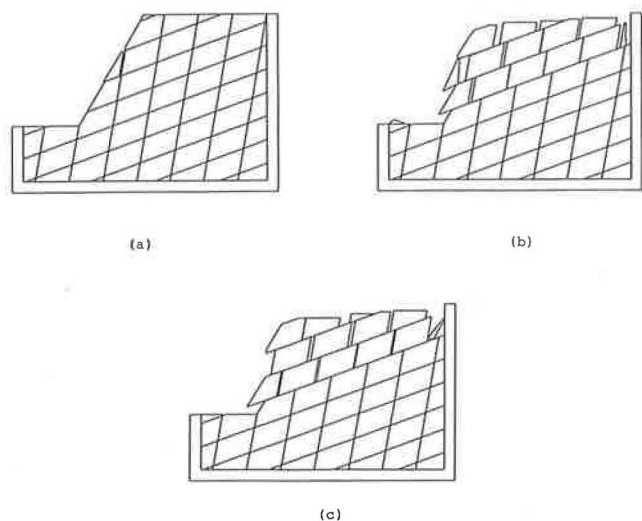


FIGURE 14 Equilibrium block positions 50 sec after earthquake: (a) scaling factor = 0.1, (b) scaling factor = 0.5, and (c) scaling factor = 0.6.

proximation. Response within each block can then be represented as a elastic-plastic material with failure defined by a Mohr-Coulomb criterion.

Formulation for Block Deformability

Fully deformable blocks are discretized into a mesh of triangular finite-difference zones, as in standard continuum modeling. Details of the formulation for fully deformable blocks are given in Board (3), Lemos (7), and elsewhere. The accuracy of the internal stress analysis corresponds to the degree of mesh refinement. Within each zone, a state of constant strain (stress) is assumed. Therefore, block boundaries remain defined by straight piecewise lines, permitting a simple determination of the relative displacements between adjacent blocks. Gridpoints are located at the vertices of each triangular zone. Their accelerations (\ddot{u}_i) are obtained from the equations of motion (no damping).

$$\ddot{u}_i = \frac{\int_S \sigma_{ij} n_j ds + F_i}{m} + g_i \quad (10)$$

where

S = Voronoi polygonal surface surrounding each gridpoint,

σ_{ij} = stress tensor,

n_j = components of the unit normal to S ,

ds = incremental surface length,

m = mass lumped at each gridpoint, and

F_i = forces that include applied external loads and contact forces if gridpoints are located on a block boundary.

Illustrative Example

Rockeries (or rockery walls) are used to provide stability to otherwise oversteep-cut and embankment-filled slopes. They consist of large individual blocks stacked to form a retaining structure, as shown in Figure 15. Use of the distinct element method to analyze the capacity of such slopes is described by Lorig and Santurbano (13) and Santurbano (14).

Figure 16 shows the problem geometry used to idealize a bridge abutment similar to that shown in Figure 15. In Figure 16, the rockery is represented by five quadrilateral rigid blocks of regular shape. The footing is assumed to consist of a single rigid block. The base of the model, which is assumed to be a firm foundation, is also represented by a fixed rigid block. The rockfill is represented by five deformable blocks that have been internally discretized with four different element sizes, on the basis of their position. The smallest mesh size is under the footing; it was determined from sensitivity studies of a footing on a frictional material. The mesh size of the region just beneath was chosen from sensitivity studies of a slope in a frictional material. A coarser mesh was selected to represent the backfill because the stress and displacement gradient expected there are less. Finally, the position of the right-hand boundary was located at a distance remote enough to eliminate its influence on bearing capacity results.

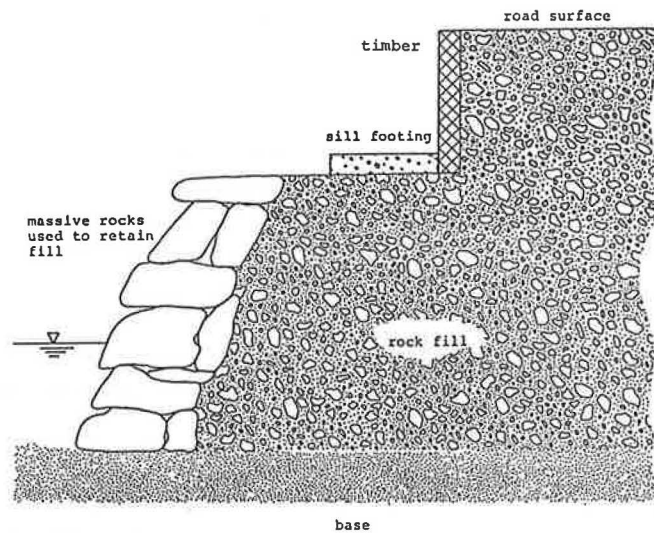


FIGURE 15 Composition of typical rockfill slope.

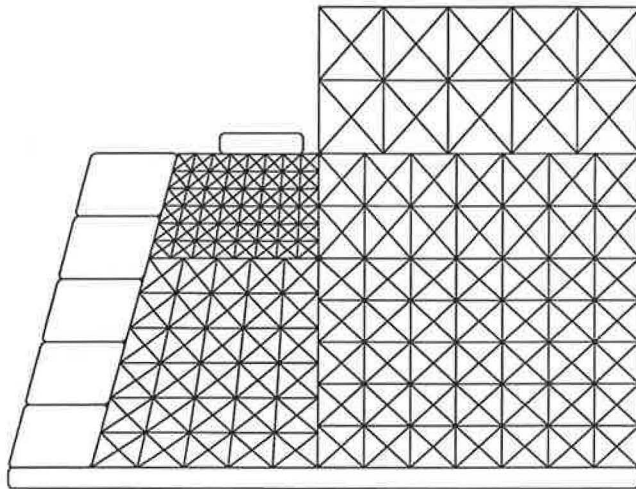


FIGURE 16 Idealization of typical bridge abutment (rockfill represented by constant strain triangular finite-difference zones).

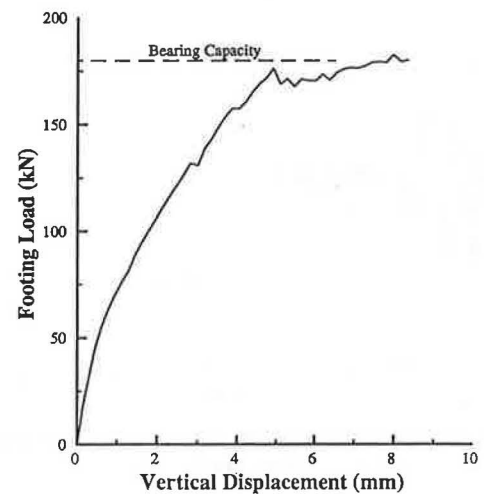


FIGURE 17 Footing load-displacement relation determined from distinct element analysis.

The footing load was simulated by applying a constant downward velocity to the rigid block representing the footing. The bearing capacity was determined by monitoring the force change beneath the footing. Figure 17 shows the relation of footing displacement and applied load. The velocity field shown in Figure 18 indicates that failure in this case results from rotation of the rock face about the base of the retaining structure; a different mode of failure, involving translational sliding, occurs for other combinations of parameters.

DISCUSSION OF RESULTS

The distinct element method provides a useful tool for understanding a wide range of problems involving the stability of slopes in jointed rock masses. The method requires specification of the usual problem parameters: geometry, joint strength properties, material density, and gravity. In addition, the

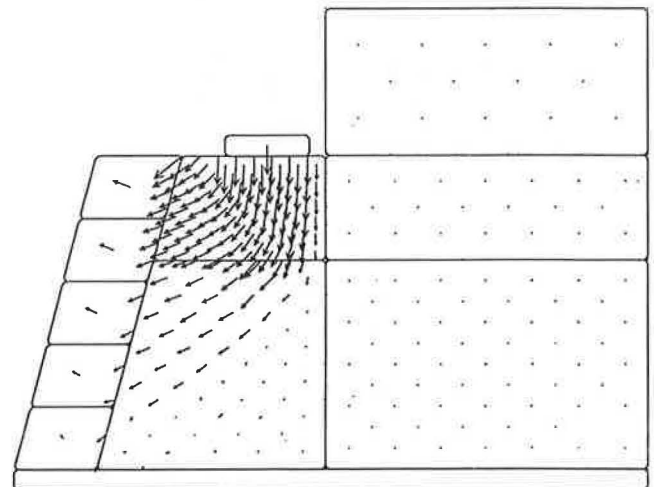


FIGURE 18 Velocity field at failure.

method uses joint stiffness properties that are difficult to determine. However, for nearly all problems, results of stability analysis are insensitive to the choice of joint stiffness. This is understandable, because stability depends primarily on strength, not on elastic properties. This paper has shown that the distinct element method overcomes the two main limitations of the limit equilibrium method, namely, the requirement to predefine the failure mode and the inability to compute displacements. The ability to estimate displacements has been shown to be particularly important for studying the behavior of rock reinforcement and rock slopes subjected to earthquake loading. Extensions of the method to include the presence of water in joints and block deformability have also been presented.

ACKNOWLEDGMENTS

The illustrative problem discussed under block deformability was studied under a contract administered by FHWA. The senior author expresses thanks to Carol Seitz of Region 10, U.S. Department of Agriculture, Forest Service, and to Al DiMillio of Office Engineering and Highway Operations R&D, FHWA, for enthusiastically sharing their time and suggestions during the course of this work.

REFERENCES

1. P. A. Cundall. A Computer Model for Simulating Progressive Large Scale Movements in Blocky Rock Systems. *Proc., Symposium of the International Society for Rock Mechanics*, Vol. 1, Nancy, France, 1971.
2. P. A. Cundall. Computer Interactive Graphics and the Distinct Element Method. *Proc., ASCE Speciality Conference*, Vol. II, Boulder, Colo., Aug. 1976.
3. M. Board. *UDEC Version ICG1.5*. Report NUREG/CR-5429, Vol. 1-3. U.S. Nuclear Regulatory Commission, Washington, D.C., Sept. 1989.
4. R. Hart, P. A. Cundall, and J. Lemos. Formulation of a Three-Dimensional Distinct Element Model—Part II: Mechanical Calculations for Motion and Interaction of a System Composed of Many Polyhedral Blocks. *International Journal of Rock Mechanics and Mining Sciences & Geomechanics Abstracts*, Vol. 25, 1988, pp. 117-126.
5. P. A. Cundall. Distinct Element Models of Rock and Soil Structure. *Analytical and Computational Methods in Engineering Rock Mechanics* (E. T. Brown, ed.). George Allen and Unwin, London, England, 1987, pp. 129-163.
6. P. A. Cundall and J. V. Lemos. Numerical Simulation of Fault Instabilities with a Continuously Yielding Joint Model. *Rockbursts and Seismicity in Mines* (C. Fairhurst, ed.). A. A. Balkema, London, England, 1990, pp. 147-152.
7. J. Lemos. *A Distinct Element Model for Dynamic Analysis of Jointed Rock with Application to Dam Foundations and Fault Motion*. Ph.D. thesis. University of Minnesota, Minneapolis/St. Paul, June 1987.
8. B. Brady and L. Lorig. Analysis of Rock Reinforcement Using Finite Difference Methods. *Computers and Geotechnics*, Vol. 5, No. 2, 1988, pp. 123-149.
9. S. Bjurström. Shear Strength of Hard Rock Joints Reinforced by Grouted Untensioned Bolts. *Proc., 3rd International Congress on Rock Mechanics*, Vol. 2, 1974, pp. 1,194-1,199.
10. P. J. N. Pells. The Behaviour of Fully Bonded Rock Bolts. *Proc., 3rd International Congress on Rock Mechanics*, Vol. 2, 1974, pp. 1,212-1,217.
11. N. M. Newmark. Fifth Rankine Lecture: Effects of Earthquakes on Dams and Embankments. *Geotechnique*, Vol. 15, No. 2, 1965, pp. 139-159.
12. J. V. Lemos and P. A. Cundall. Earthquake Analysis of Concrete Gravity Dams on Jointed Rock Foundations. *International Journal for Numerical and Analytical Methods in Geomechanics* (in preparation).
13. R. Santurano and L. Lorig. An Improved Procedure for Design of Rockeries Using ESAC. *Rock Mechanics Contributions and Challenges*, A. A. Balkema, Rotterdam, the Netherlands, 1990, pp. 769-776.
14. R. Santurano. *Development of a Computer-Aided Design Procedure for Massive Rock Slope Stability Analysis*. M.S. thesis. University of Minnesota, Minneapolis/St. Paul, 1990.

Publication of this paper sponsored by Committee on Soil and Rock Properties.